Phase formation and magnetic properties of nanocrytalline Ni70Co30 alloy prepared by mechanical alloying

Nadia Loudjani, Takrim Gouasmia, Mohamed Bououdina, Jean-Louis Bobet

Phase Formation and Magnetic Properties of Nanocrytalline $Ni_{70}Co_{30}$ Alloy Prepared by Mechanical Alloying

N. Loudjani [1], T. Gouasmia [2], M. Bououdina [3 *], J. L. Bobet [4]

[1] Laboratoire de Microstructures et Défauts, Department of Physics, College of Science, Brothers Mentouri University, 25000, Constantine, Algeria

[2] Laboratoire de Développement des Énergies Nouvelles et Renouvelables dans les Zones arides et Sahariennes, Department of Physics, College of Science, Kasdi Merbah University, 30000, Ouargla, Algeria

[3] Department of Physics, College of Science, University of Bahrain, P.O. Box 32038, Bahrain

[4] University of Bordeaux, CNRS, Bordeaux INP, ICMCB, UMR 5026, F-33600, Pessac, France

* Corresponding author: mboudina@gmail.com (Mohamed Bououdina, PhD)

Abstract

Nanocrystalline $Ni_{70}Co_{30}$ alloy was synthesized by high energy ball alloying from elemental pure Ni and Co powders as function of milling time. The changes in structural, morphological and magnetic properties of the processed powders during mechanical alloying were characterized respectively by X-ray diffraction, scanning electron microscopy and vibrating sample magnetometer. X-ray diffraction analysis suggested the formation of two fcc nanostructured solid solutions fcc-Co(Ni) and fcc-Ni(Co), where the crystallite size decreases reaching 4.7 – 8.0 nm while the microstrain increases up to 0.39 - 0.42%, due to the severe plastic deformations and the structural defects introduced by milling. Morphological observations indicated a progressive refinement of the particles size with milling time. For longer milling, a narrow particle size distribution with irregular shape was observed. Milling process induced some important changes in the magnetic properties, whereas the variation of the saturation magnetization and coercivity was associated mainly to the particle size refinement, accumulation of microstrain and formation of solid solutions Co(Ni) and Ni(Co).

Keywords: *Mechanical alloying; Nanostructures; $Ni_{70}Co_{30}$, Solid solution; Magnetic properties.*

1. Introduction

Nanomaterials (NMs), described as non-equilibrium materials with new performances, have become the most developed and promising field of materials science and engineering. Compared to traditional counterparts, NMs of similar compositions display enhanced and superior properties, which offers possibilities for modern technological applications in everyday products **[1-2]**. In fact, the combination of grains/particles at the nanometer size, the high surface area, and the superior directionality enables nanostructures to access into interesting ranges of mechanical, electronic, optical or magnetic properties **[3].** It has been reported that these properties depend mainly on the individual crystalline particles and particle boundaries including chemical composition, structure, size and shape **[3]**. Therefore, extensive researches have been conducted in order to understand their behavior and consequently to control their properties using advanced characterization techniques and modeling.

Soft magnetic nanomaterials (SMNs) have known increasing attention in the past years due to their common and unique characteristics to both amorphous and crystalline materials that provide many exciting opportunities in magnetic applications. SMNs exist in different forms, including nanoparticles, nanostructured thin films, nanowires, nanocrystalline ribbons, and so on. They can be employed in a variety of devices such as transformers, motors and generators conversion of electrical energy **[4]**.Such applications require a combination of high magnetic flux density, high permeability, and a reduced coercive force **[5]**. It is well-known that the decrease of grain size to the order of the domain wall exchange length lowers the coercivity towards a value controlled by the random anisotropy model **[6]**.The production of such forms of SMNs was possible, via chemical synthesis, plasma processing, or mechanical alloying (MA) **[4]**.

Recently nanocrystalline soft magnetic materials synthesized by MA have experienced a large development **[7]**. The reduction of particle size by MA to the nanoscale usually accompanied by important modifications in the magnetic behavior and properties of powders that remain strongly correlated to both phase and chemical composition as well microstructure such as particle size distribution, internal tension, and the anisotropically shaped particles **[8]**.

It has been noted that with MA it is easier to obtain the materials far from their thermodynamic equilibrium. In particular, extended solid solutions, nanocrystalline, quasicrystalline, and amorphous alloys with a large difference in melting temperatures of its ingredient can be obtained via MA. Because of the chemically randomizing nature of MA, it can force heterogeneous elements into a homogeneous amorphous alloy at room temperature **[9].**

During MA process, particles are subjected to severe plastic deformations. It consists of a repeated fracturing and cold-welding of particles leading to significant size refinement of the powder particles and a change in their shape **[10]**.

Co-Ni nanoalloys were synthesized by different methods such as MA, polyol reduction and sol-gel methods have been widely reported in the literature **[11]**. They showed a typical soft ferromagnetic behavior because of their new anisotropic shape. Aymard et al. **[12]** synthesized and characterized the microstructural and magnetic properties of Co-Ni alloys prepared by MA with various compositions; the milling was carried out in a SPEX 8000 mill under an argon atmosphere. The analysis of X-ray diffraction showed: (i) an allotropic transformation of Co from hcp form to fcc during the first stage of milling, (ii) a mutual diffusion of Ni and Co into each other leading to the formation of two phases with fcc structure. The obtained milled powders exhibited a nanocrystalline character with a high rate of micro deformations. The measurement of the saturation magnetization and the coercivity performed for $Co_xNi_{100\_x}$ alloys (x = 30, 50, 70)

indicated that the oxygen contamination decreases the value of the saturation magnetization by 15%. Over the past decade, Loudjani et al. devoted numerous studies about Co-Ni alloys during high energy milling **[10, 13-15]**. The obtained results indicated the formation of homogeneous solid solutions (SS) with a high rate of microstrain. The solid solution structure was either fcc, hcp or mixed fcc and hcp. It was found that the structure depends essentially on the shape and the size of milled particles as well as the percentage of Co in the alloy. The intensive generated energy during milling process induces the diffusion of Co and Ni atoms in the SS phases and the allotropic transformation of Co. It was also found that milling affects significantly the magnetic properties. In fact, the variation of coercivity (H_c) and saturation magnetization (M_s) of CoNi alloys could not be predicted; i.e. $Ni_{50}Co_{50}$ **[14]** and $Ni_{20}Co_{80}$ **[10]** showed different behaviors: $Ni_{50}Co_{50}$ alloy reached H_c of 34.5 Oe and M_s of 150.3 emu/g **[14]** while $Ni_{20}Co_{80}$ exhibited higher Hc (60 Oe) and lower Ms (125 emu/g) **[10]**. The common conclusion was that the alteration of the magnetic parameters was related to crystallite size, phase and chemical composition, microstrain, and the formed solid solutions.

In the case of polycrystals, in order to improve the properties of Co-Ni alloys, other elements are added to the binary alloys such as Fe, Ga, and Cu. For example, the Co-Ni-Ga alloy has been investigated; the study was devoted to the magnetic properties of $Co_{36.4+\ x}Ni_{33.3\ -\ x}Ga_{30.3}$ system obtained by melting under controlled Argon atmosphere **[16]**. The magnetic hysteresis cycles obtained for four compositions ($0 \leq x \leq 3.1$ at.%) exhibited very narrow hysteresis loops. From the above studies, it can be highlighted that the maximum magnetization of the studied alloys increases with the amount of Co. Likewise, the coercivity increases with the content of Co; it has a greater value for compositions with Co above 39.5 at.%. This behavior has been attributed to the increase

in magnetic anisotropy with the proportion of Co. Similar results have been also observed on nanocrystalline alloys obtained by mechanical grinding of the ternary alloys CoNiFe **[17].**

This research work aims to investigate specifically the binary $Ni_{70}Co_{30}$ alloy prepared by high energy ball milling, since to the best knowledge of the authors, no studies are reported in the literature. Particular emphasis will be devoted to the effect of milling on structural and magnetic properties of this alloy as well as the influence of Ni that favors the development of metastable structures at low milling times. This paper presents the evolution of phase formation and composition, structural and microstructural parameters as well magnetic properties of mechanically alloyed $Ni_{70}Co_{30}$ powder mixture as function of milling time.

2. Experimental details

A. Mechanical alloying of $Ni_{70}Co_{30}$ powder mixture

The preparation of $Ni_{70}Co_{30}$ powders was carried out by mechanical alloying using a planetary mill type Pulverisette P5. The synthesis was performed by cycles of 30 min of milling at 250 rpm followed by 15 min pause to avoid an excessive rise in temperature inside the vials. For each powder, a mass of 8 g was crushed under an argon atmosphere, in vials containing 36 instrumented steel balls of 1 mm in diameter, the ratio of the mass of the balls and the mass of the powder being equal to 17: 1.

B. Characterization of mechanically alloyed $Ni_{70}Co_{30}$ samples

The samples were characterized by X-ray diffraction (XRD) using a Philips PANalytical X'Pert (PW1820) diffractometer equipped with Cu $K_{\alpha 1}$ radiation source (λ=1.5418 Å). The amount of each phase was estimated from XRD refinement using EVA software.

The average crystallite size (D) and microstrain (ε) were determined by using the following equations **[9]**:

$$D = \frac{0.9\,\lambda}{\beta\cos\theta} \qquad (1)$$

$$\varepsilon = \frac{\beta}{4\tan\theta} \qquad (2)$$

where λ is the wavelength of the X-ray radiation, θ is the diffraction peak's position, and β is the full width at half maximum (FWHM). Instrumental broadening corrections were performed using a LaB6 standard.

Morphology observations of the milled powder mixture (changes in shape, size, particle size distribution) were carried out by scanning electron microscopy (SEM) using a Zeiss DSM 960A microscope operating at voltage of 20 kV and equipped with electron dispersive X-ray (RDS) detector for chemical analysis.

Magnetic measurements were carried out at room temperature using a vibrating sample magnetometer (VSM) MicroMag model 3900 with a maximum magnetic field of 10 kOe (1 Tesla).

3. Results and Discussion

3.1 XRD Analysis

3.1.1 Evolution of Phase Composition

The evolution of XRD patterns with milling time is displayed in Fig. 1. The XRD pattern of the un-milled powder mixture shows the presence of characteristic peaks of face centered cubic Cobalt (fcc-Co), hexagonal close packed Cobalt (hcp-Co) and face centered cubic Nickel (fcc-Ni). The main peaks are indicated by the plans (111), (200) and (220) for fcc phase as well (100), (002) and (101) for hcp phase (Fig. 2). As a consequence of their close lattice parameters, the resolution of both elements was prevented. In addition to the identified peaks belonging to both Co and Ni, few

additional minor peaks with low intensity probably related CoO and/or NiO oxides are detected. The observed slight shift of the main Ni and/or Co diffraction peaks towards smaller 2θ angles can be correlated to the lattice distortion of Ni and/or Co arising from their interdiffusion.

As a result of the progressive mixing of cobalt (Co) and nickel (Ni) powders as well due to the severe plastic deformations caused by the high energy ball milling, many phenomena take place. As milling proceeds, the crystallite size decreases while the atomic level of strains rises continuously. A variety of crystal defects such stacking faults, dislocations, vacancies and grain boundaries are introduced promoting the mutual diffusivity of both elements during the milling process. The effect of such phenomena can be observed clearly on the diffraction peaks illustrated in Fig. 1. The intensity of diffraction peaks reduces gradually although their width increases with the milling time, indicating the evolution of phases besides grain refinement and higher defects density.

After 1h of milling, the same peaks are observed as in the un-milled mixture (0h) with a small decrease in intensity especially for (101) line of hcp Co phase (Fig. 2). This line disappears completely after 4 h of milling while the peaks related to the lines (111) and (200) of fcc Co phase remain present with a notable decrease in their intensity. This can be attributed to several reasons such as reduction in particle size, the dissolution of Co into Ni lattice or the reverse allotropic phase transformation of Co from hcp to fcc **[14]**.

One of the most important features of the binary CoNi alloys is the appearance of the reversible phase transition of Co phases as shown in the phase diagram **[18, 19]**. The temperature of this phase transformation decreases when the rise in Ni content. The allotropic transformation of Co during the mechanical alloying of elements has been reported in the literature **[13-15]**. At ambient

temperature, Co phase is considered as a metastable structure and due to external energy either mechanical or thermal **[19]**. Besides, the milling time and intensity are considered as major factors of the allotropic phase transformation of Co **[20]**. It has been deduced that for short milling time and higher milling intensity, this transformation is faster **[21]**. Many studies also **[10,23]** confirmed that while milling time increases, a large amount of stacking faults accumulated within the hcp-Co lattice inducing the hcp-Co phase transformation into fcc-Co phase. Further, this phase transition can be favored by the contamination of the hcp-Co powder by Fe originating from bowl and balls, leading to the stabilization of the fcc-Co form **[22]**.

In their study; Cardellini et al. **[20]** pointed out that it is essential to take into consideration Fe contamination during the transition of cobalt structures; Fe stabilizes the fcc-phase of Co at room temperature up to 5 at.% content following the standard phase diagram.

For longer milling times (5, 10, 15 and 25 h), a significant reduction of diffraction peaks intensity is observed. It is obvious that the line profiles are almost symmetrical which is related to the formation and the stabilization of a new phase, identified as a solid solution of two fcc structures of Ni and Co. The phase diagram of Co and Ni alloys **[18]** indicates that at temperatures between the solidus and the allotropic transformation, Co and Ni can form a complete solid solution with an fcc structure; this transformation takes place at a temperature close to 300°C **[18]**. One of the most known fcc high-temperature phase is the $Co_{84.43}Ni_{15.57}$ alloy **[22]**.

According to Hume-Rothery rules, a solid solution is favorable following 4 conditions: (i) the difference in atomic radii is less than 15 %; (ii) both elements have same crystal structures; (iii) close electronegativity; and (iv) same valence. For the $Ni_{70}Co_{30}$ alloy, the above criteria are fulfilled, therefore the formation of heterogeneous solid solution is likely occur: very close atomic

radii of Ni and Co (0.124 nm and 0.125 nm respectively), fcc-Ni and of course the Co-fcc obtained after phase transformation, both Ni and Co have an electronegativity of 1.9 and same valence of +2. Therefore, Co-Ni alloy formation occurs simultaneously during the conversion of hcp-Co form into fcc form and the mutual diffusion of Co and Ni in the two fcc phases. The existence of the fcc-Ni(Co) and the fcc-Co(Ni) solid solutions is confirmed by the important decrease of Ni and Co peaks intensities after 5 h. It is important to mention that because of the larger diffusivity of Co into Ni lattice ($D = 2.51\times10^{-8}$ m^2/s at T=800°C) than that of Ni in Co ($D = 1.02\times10^{-8}$ m^2/s at T=800°C) **[23]**, the proportion of the fcc-Ni(Co) solid solution is found more noticeable than that of fcc-Co(Ni).

Many previous studies reported that during MA a non-homogeneous solid solution can be formed by the diffusive mixing process in binary alloys **[7,15,24]**. As it was confirmed by XRD patterns **[10,13-15],** the Co-Ni alloys prepared by MA are nanocrystallized solid solutions. In the $Co_{50}Ni_{50}$ alloy **[13, 14]**, the formation of grain boundaries in the milled elements facilitates the diffusion of Co and Ni into each other region, resulting in the creation of two main solid solutions: dominant fcc-Ni(Co) and fcc-Co(Ni). For the $Co_{80}Ni_{20}$ alloy **[10]**, several solid solutions with different structures were detected through XRD analysis. In addition to the two fcc solid solution phases detected in $Co_{50}Ni_{50}$ powder mixture, a new solid solution with an hcp structure (hcp-Co(Ni)) was identified. The same mixture of fcc and hcp solid solutions was observed in the milled $Co_{90}Ni_{10}$ **[25]**.

3.1.2 Microstructural Study

The formation of solid solution (SS) as confirmed by the change in XRD peaks broadening has been accompanied by particle size reduction (grain refinement) and the increase of lattice microstrain. Both parameters are essential to follow the phase constitution and transformation

characteristics during high energy milling. Both microstructural parameters have been calculated using the widening of XRD peaks by taking into consideration instrumental contribution. Fig. 3 depicts the evolution of crystallite sizes $\langle L \rangle$ and internal microstrain $\langle \sigma^2 \rangle^{1/2}$ for the two solid solutions fcc-Co(Ni) and fcc-Ni(Co) along various (hkl) planes as function of milling time.

It has been reported that, the progress of microstructural parameters $\langle L \rangle$ and $\langle \sigma^2 \rangle^{1/2}$ in mechanically alloyed materials peruse two main stages **[26]**: (i) during the first stage, particles refinement occurs accompanied by an increase in microstrain; while (ii) the second stage is defined by a steady-state for both parameters. Clearly, after the first 4 h of milling, the crystallite size for both SS phases decreases rapidly from 31.85 nm (0h) to 7.60 nm (4 h) for the SS of fcc-Ni(Co) and from 27.34 nm (0 h) to 6.41 nm for the fcc-Co(Ni) SS. The important grain refinement occurs with a progressive rise in microstrain level as milling time is prolonged. The rapid reduction indicates the effect of repeated collisions in flattening the grains. MA process was known by the ability to reduce particle size to the range of nanometer in a short time **[27]**. In fact, the higher the shock intensity is, the narrower the grain size. In this stage, the severe plastic deformation leads to a developing number of matrix dislocations. The created dislocations are multiplied in the shear zones. As a result of their rearrangement and interactions **[28]**, new surfaces are established leading to the phenomenon of polygonization **[15]**. Thus, the size of crystallites declines and the value of lattice microstrain rise. Since the rise in the local temperature during milling process has been reduced by applying a pause repeatedly, hence the effect of grain growth does not appear in this study, in contrary to similar work in the literature **[29]**.

At longer milling above 5 h, the variation of crystallite size and microstrain is gradually reduced. The rise of surface temperature during MA process could be the origin associated with this modest variation of both parameters **[30]**.

The evolution of crystallite size afterward remains stable; reaching about 8 nm and 4.67 nm after 25 h for fcc-Ni(Co) SS and fcc-Co(Ni) SS, respectively. It is important to mention that for prolonged periods of milling (15 and 25 h); the sub-grains are disoriented one to another. Thus, the deformation occurs mainly on grain boundaries. This phase stabilization can be associated with the constraint of the crystallites deformation σ_p defined by Hall-Petch relation **[31, 32]**, which becomes much superior to that caused by milling. The new surfaces created previously cannot be formed again considering that grains attain their size limit improving the inversely proportional relation between strength and crystallite size as described by Hall-Petch relation. The reached value of $\langle L \rangle$ can be correlated with an equilibrium state of the $Ni_{70}Co_{30}$ mixture. The possible explanation is that when this critical value is achieved, the required energy to create further deformations, new grain boundaries and interfaces appears to be too high **[33]**.

On the other hand, the increment of microstrain level continues moderately until reaching a maximum value of 0.39% for fcc-Ni(Co) SS and 0.42 % for fcc-Co(Ni) SS. This is due to the high density of dislocations produced by severe plastic deformations of high energetic nanoparticles for longer milling times, which shows the anisotropic behavior **[14]**.

The calculated microstrain values are comparable to those found for other ball-milled metals and alloys. In particular, the fcc-Ni(Co) phase of the milled $Co_{50}Ni_{50}$alloyshowed a microstrain rate of 0.31% after 24 h of milling which is close to that of $Ni_{70}Co_{30}$ alloy while the fcc-Co(Ni) phase of the same alloy **[14]** displayed twice (0.85%) the microstrain rate of that in $Ni_{70}Co_{30}$ alloy. From this comparison, one can conclude that due to the fragile nature of Co particles comparable to that of Ni, Co(Ni) phase possesses the highest deformation values, hence the smallest crystallite size **[34,35].**

3.2 SEM Analysis

SEM micrographs of $Ni_{70}Co_{30}$ alloys obtained at various milling durations (0 – 25h) are shown in Fig.4.It can be noted the existence of gradual grains refinement with milling time. The morphology presented in Fig.4. $Ni_{70}Co_{30}$ powder mixture before milling shows two different types of particles: smooth rounded spherical particles belonging to Ni powder and rough bulky particles consist of several smaller particles belonging to Co powder. In view of the magnetic nature of both Co and Ni, many blocks of agglomerated particles can be observed in the unmilled $Ni_{70}Co_{30}$ alloy morphology.

After the first hour of milling (1 h), notable microstructural modifications occur and new surfaces are formed. This is can be related mainly to the different mechanical properties of both metals: Ni is a rigid, ductile and malleable metal so the atoms tend to enter new positions without destroying the metallic boundary, while Co is hard and fragile. Consequently, the particles are smashed and transformed into an irregular shape with a heterogeneous size distribution. Therefore, a mixture of large and small particles is observed along this phase of MA (Fig. 4). The variation of morphology and particle size originates from combined three principal mechanisms: plastic deformation, cold welding, and fracturing. The particles are agglomerated, fractured progressively into fragile flakes by the compressive forces generated during the balls-powders collisions, and then they are cold-welded, agglomerated and de-agglomerated. During MA, these mechanisms compete and control the morphology of powders during different alloying periods. Because of the ductility of both Co and Ni, the diffusivity of their particles in each other lattice is favored and the particle size rises in early milling stages (5 h). According to Suryanarayana **[27]**, particles of ductile-ductile alloyed systems can be plastically deformed smoothly; they are flattened, cold-welded, fractured then they rewelded.

Besides, the soft particles activated by the newly created surfaces tend to aggregate and create larger particles by cold welding. Thus, the welding process is dominant at this stage of milling. The $Ni_{70}Co_{30}$ alloy presents a structure of large sharp edges particles as it is shown in Fig. 4.

For relatively longer milling time (10 h), fracturing becomes the most predominating process assuming the brittle property of Co particles. Thus, the mechanism of fracture tends to generate fragments of powder particles that continue to decrease gradually in size because of the lack of active agglomerating forces.

Milling extended up to longer durations (15 and 25 h) results in the formation of more homogenous powders mixture with irregular shape and reduced particle size.

One can notice that the edges are gradually fractured and particles share and size become more refined (Fig. 4). The nearly uniform size distribution of particles is a result of severe deformations and cold welding; the large particles are fractured into small ones although the smaller particles are welded to each other **[36, 37]**. In addition, the powder morphology is characterized by a matrix of thin layers of highly deformed particles randomly welded. Therefore, one can deduce that the lamellar-type microstructure formed between Co and Ni is mechanically preferred. Considering that this lamellar phase is very reactive, the diffusivity of Co and Ni elements is enhanced. Many studies **[38-40]** confirmed that these lamellar multilayer structures are usually formed in ductile-ductile mechanically alloyed systems, as a result of the combination of frequent mechanical deformations and cold welding. The micrograph of milled powders for 25h illustrates the competition between the two mechanisms of hard deformations and welding. As it is observed, both fine particles and agglomerates coexist. Thus, a relative equilibrium of cold welding and fracturing is reached at this point of milling. However, several regions possess a modest growth of

particles. This can be justified by the incorporation of fine particles into the layered matrix and/or the welding of fragments together.

3.3 Magnetic Properties

In order to examine the effect of MA on the magnetic behavior as well the evolution of magnetic properties of $Ni_{70}Co_{30}$ alloy selected samples, the hysteresis loops have been recorded as illustrated in Fig. 5. The nanostructured $Ni_{70}Co_{30}$ milled alloys show similar and sigmoidal small hysteresis cycle which indicates their typical ferromagnetic order. Generally, fine soft magnetic materials possess a small coercive domain (narrow hysteresis loops) **[41]**. This behavior can be related mainly to the microstructural internal deformations. The magnetization-field (M-H) loops have been used to determine the values of the coercive field (H_c) and the saturation magnetization (M_s) at various milling durations. The evolution of H_c and M_s with alloying time is displayed in Fig. 6.

Since, the magnetization process depends essentially on the movement of domain walls and the rotation of spin; hence it can be strongly influenced by the grain refinement. Thus, the following reasons can be the origin of the variation of coercivity and magnetic saturation: crystallite size, the lattice internal strain, the density of defects, the domain walls displacement and the redistribution of elements during phase evolution **[6]**.

The curve of coercivity H_c shown in Fig. 6a can be divided into three main stages.

The first stage shows a slight increase in coercivity from 62.65 Oe to 76.65 Oe after 1 h of milling. A high value of H_c indicates the existence of micro-deformations, impurities, pores and various defects that can appear during the milling process. Actually, as the magnetization reverses, the severe plastic deformations and the various defects generated by the repeated collisions ball-powder and/or ball-powder-wall of the milling bowl serve to trap the walls of magnetic domains

during their movements **[42,44]**. Hamzaoui et al. **[45]** followed the evolution of H_c as function of collision power. It was deduced that the introduction of high internal stains caused the increase of this magnetic parameter. The magnetic domain walls can be pinned to another anisotropic ferromagnetic particle and/or non-magnetic inclusions causing the increase of H_c **[46]**. This modest increase of coercivity can be also caused by the simultaneous diffusion mechanism, the allotropic transformation of Co as well the formation of solid solution at the same time. Further, it can be resulted by the irregularities of the newly created surfaces and/or the random shape of particles **[47-48]**. Similar rise in H_c was observed for the $Ni_{60}Cr_{40}$ alloy upon 3 h of milling; from 19 to 60 Oe **[49]**.

The second interval exhibits a rapid reduction of coercivity up to 4 h, from 76.68 Oe (1h) to 31.21 Oe (4 h). During this milling period, the shape of particles changes gradually from a lamellar to a spherical, leading to the reduction of the anisotropy related to the shape **[47, 50, 51]**. Due to the progressive powders diffusivity, the mixture becomes more homogeneous and the grains are refined. As a consequence, the magnetocrystalline anisotropy is reduced. In fact, it was deduced that for soft nanocrystalline magnetic materials, when the grain size is reduced to about 6 nm, to the order of the ferromagnetic exchange length, the magnetic anisotropy level became average and the coercive field H_c decreases proportionally with the grain size **[52]**. Therefore, the magnetic characteristics become softer. The milled $Ni_{70}Co_{30}$ alloy was identified previously by the allotropic transformation of Co which can affect the coercivity because of the continuous disappearance of the hcp-Co phase in favor of the fcc-Co phase. It was well established that the Co-fcc structure possesses smaller magnetocrystalline anisotropy than Co-hcp **[53]**. Thus, this reduction of coercivity occurs simultaneously with the formation of the alloy. The dislocation density as well was considered as a principal parameter influencing the coercivity **[54]**. The entanglements of

dislocations generate barriers that prevent the plastic flow of the material and tend to interact strongly with the walls of the magnetic domain in ferromagnetic materials **[55]**. The discontinuous movement of domain walls which are fixed by dislocations tangles and other inhomogeneities create a change in the magnetic flux density **[55]**. The decrease of particle size resulting from the competition between fracture and welding can be also related to the coercivity. Similar behavior was observed in FeNbB alloy obtained by mechanical milling **[56]**. Both, $Co_{80}Ni_{20}$ **[10]** and $Co_{50}Ni_{50}$ **[14]** milled alloys showed a rapid decrease in coercivity after 3 h of milling.

In the third region, a slight increase to 32.35 Oe is noted followed by a steady state on prolonged milling time, which can be related to the effect of the very small crystallite size. In this case, the high level of microstrain impacts the coercive field much more than the crystallite size, hence confirming the theory of soft magnetic materials **[14, 57,58]**. The crystallites are very small at this level and the nanostructured alloy transformation is completed, leading to a decrease in coercivity. Because of their important density in the particles during this milling stage, dislocations are annihilated and H_c is reduced. Another explanation is the minimization of surface irregularities as function with milling time **[47]**. The values of Hc obtained after 25 h for milling is comparable to the value 34 Oe found in the $Co_{50}Ni_{50}$ powders prepared by MA **[14]**.

The change of saturation magnetization M_s with milling time as shown in Fig. 6b exhibits an antagonistic behavior. The value of M_s increases gradually from 76 emu/g up to a maximum of 107 emu/g after 15h of milling, then decreases sharply to 87 emu/g after 25h. The milled $Co_{50}Ni_{50}$ **[14]** and $Fe_{50}Co_{40}Ni_{10}$ **[59]** alloys showed similar trend for 24 and 90 h of MA respectively while the $Co_{80}Ni_{20}$ **[10]** alloy had an opposite trend up to 12 h of milling. After the first 3 h of milling, M_s decreased from 147 to 130 emu/g and then increased to 135 emu/g for 12 h. Up to 48 h of milling, the M_s of $Co_{80}Ni_{20}$ continued to decrease until reaching a value of 127 emu/g.

The increase of M_s during the first 15 h of milling process can be attributed to the combined effects associated with the formation of solid solutions and the refinement of microstructure. In fact, in correlation with XRD analysis (Fig.1), the formation of two different solid solutions fcc-Co(Ni) and fcc-Ni(Co) by diffusion mechanism has been confirmed during early hours of MA. This diffusion induces the transformation of charges between the atoms of the two ferromagnetic elements **[59]**.

Further, the diminution in the anisotropy of magneto-crystalline caused by the gradual reduction of crystallite size tends to facilitate the rotation of the magnetic vector **[10]**. At this stage of milling, the averaging impact of the magnetization dominates the random orientation of nanocrystalline powder and the possibility of considering each grain as a single magnetic domain eliminates the magnetic wall effect **[10, 14, 60]**. It is important to mention that for the $Ni_{70}Co_{30}$ alloy, the continuous substitution of Ni atoms in the solid solutions improves the alloying completion and particles refinement, as confirmed in several studies in the literature **[10,61,62].**

Moreover, the change in the lattice parameter of milled alloys was considered also as a factor of the observed increase in M_s value. This contribution can be caused by the alloy formation, the created order-disorder and the high level of defects especially antisites that generate several alterations in the electronic band arrangements **[63]**.

Along the milling process, a large disorder of atoms is generated resulting in a significant modification in the magnetic moment. Because of the change in the configuration of the magnetic elements (Ni and Co), the magnetic atoms are arranged in the highly disordered grain boundaries. In fact, the disordered imperfections such as dislocations and grain boundaries accompanied by the important internal strain induced by MA block the movement of magnetic domain walls.

Hence, the magnetic saturation decreases. The fact that M_s reduces with particles refinement can be ascribed to the existence of an inert or no-functional surface layer that has a small magnetization **[14, 64]**. It is probable that after 15h of milling, the formation of a non-magnetic intermetallic alloy can contribute in the decrease of magnetization saturation.

One can conclude that the saturation magnetization increases with longer milling time, while the coercivity decreases. By comparison with XRD analysis, this result can be attributed to the crystallite size refinement as consequence of milling. This variation with crystallite size is also explained on the basics of domain structure, mean size of particles and crystal anisotropy.

Since milling time causes changes by decomposition or transformation of phases, as consequence there is an increase in the crystallite size, decrease of microstrain and subsequently a reduction in the value of coercivity **[10, 14].**

4. Conclusion

The effect of MA on the evolution of structural, morphological and magnetic properties of mechanically alloyed $Ni_{70}Co_{30}$ alloy prepared from elemental Ni and Co powders has been investigated. XRD analysis indicates the formation of two main solid solutions Co(Ni) and Ni(Co) with a face centered structure. This phenomenon was confirmed by the progressive decrease of peaks' intensity as well as the remarkable peak broadening with milling time. The powder-ball collisions generated severe plastic deformations and high level of crystal defects promoting the mutual diffusivity of elements. The allotropic structural transformation of Co from hcp to fcc has

been identified; hcp-Co peaks completely disappear after 4 h. Prolonged milling time procured a maximum value of accumulated strain (0.42% for fcc-Co(Ni) and 0.39% for fcc-Ni(Co)). Unlike the level of microstrain, crystallite size gradually decreases reaching 4.67 nm for fcc-Ni(Co) and 8 nm for fcc-Co(Ni). The competition between cold welding and fracturing phenomena for longer milling durations, as illustrated by SEM micrographs reveals irregular shaped particles and homogeneous size distribution with an important effect of the ductile-ductile mixture property. Magnetic measurements of the milled $Ni_{70}Co_{30}$ alloy powder exhibit a soft ferromagnetic character where the magnetic parameters are sensitive to the milling time, mainly due to the particle size refinement as well as the formation of Co(Ni) and Ni(Co) solid solutions. Both the saturation magnetization (Ms) and coercivity (Hc) are found to decrease with milling time, attaining the values of Ms = 87 emu/g and Hc = 30 Oe after 25 h of milling.

References

[1] P. G. Jamkhande, N. W. Ghule, A. H. Bamer, and M. G. Kalaskar, "Metal nanoparticles synthesis: An overview on methods of preparation, advantages and disadvantages, and applications" *J. Drug. Deliv. Sci. Technol.*, vol. 53, 2019.

[2] I. Khan, K. Saeed, and I. Khan, "Nanoparticles: Properties, applications and toxicities" *Arab. J. Chem.*, vol. 12, no. 7, pp. 908–931, 2019.

[3] M. MostafaKhalaf, H. GamalIbrahimov, and E. HummatIsmailov, "Nanostructured Materials: Importance, Synthesis and Characterization - A review" *Chem. J.*, vol. 2, no. 3, pp. 118–125, 2012.

[4] S. Lan and M. A. Willard, "Synthesis of Soft Magnetic Nanomaterials and Alloys" in *Magnetic Nanomaterials - Fundamentals, Synthesis and Applications*, 2017, pp. 121–146.

[5] G. Herzer, "Modern soft magnets: Amorphous and nanocrystalline materials" *Acta Mater.*, vol. 61, no. 3, pp. 718–734, 2013.

[6] G. Herzer, "The Random Anisotropy Model" in *Properties and Applications of Nanocrystalline Alloys from Amorphous Precursors*, 2005, pp. 15–34.

[7] Y. Xu, Y. Sun, X. Dai, B. Liao, S. Zhou, and D. Chen, "Microstructure and magnetic properties of amorphous / nanocrystalline $Ti_{50}Fe_{50}$ alloys" *J. Mater. Res. Technol.*, vol. 602, pp. 1–8, 2019.

[8] M. Khajepour and S. Sharafi, "Structural and magnetic properties of nanostructured Fe_{50} (Co_{50})–6.5wt % Si powder prepared by high energy ball milling" *J. Alloys Compd.*, vol. 509, no. 29, pp. 7729–7737, 2011.

[9] C. Suryanarayana, "Mechanical alloying and milling" Prog. Mater. Sci., vol. 46, no. 1–2, pp. 1–184, 2001.

[10] N. Loudjani, M. Benchiheub, and M. Bououdina, "Structural, Thermal and Magnetic Properties of Nanocrystalline $Co_{80}Ni_{20}$ Alloy Prepared by Mechanical Alloying" *J. Supercond. Nov. Magn.*, vol. 29, no. 11, pp. 2717–2726, 2016.

[11] S. Panday, P. Jeevanandam, and B. S. S. Daniel, "Synthesis and magnetic properties of nanocrystalline Co-Ni alloys : A review" *Mater. Sci. Forum*, vol. 736, pp. 229–240, 2013.

[12] L. Aymard, B. Dumon, "Production of Co-Ni alloys by mechanical-alloying" *J. Alloys. Compd.*, vol. 242, pp. 108–113, 1996.

[13] N. Loudjani, N. Bensebaa, S. Azzaza, J.J. Suñol and J.M. Grenèche, "Thermal and structural properties of ball milled Co_{50} Ni_{50} powders" *Matériaux. Tech.*, vol. 99, pp. 707–716, 2011.

[14] N. Loudjani, N. Bensebaa, L. Dekhil, S. Alleg and J.J. Sunõl, "Structural and magnetic properties of $Co_{50}Ni_{50}$ powder mixtures" *J. Magn. Magn. Mater.*, vol. 323, pp. 3063–3070, 2011.

[15] N. Loudjani, N. Bensebaa , S. Alleg, C. Djebbari and J.M. Greneche, "Microstructure characterization of ball-milled $Ni_{50}Co_{50}$ alloy by Rietveld method" *Phys. Status Solidi Appl. Mater. Sci.*, vol. 208, no. 9, pp. 2124–2129, 2011.

[16] A. Tejeda-Cruz, F. Alvarado-Hernández, D.E. Soto-Parra, R. Ochoa-Gamboa, P.O. Castillo-Villa, H. Flores-Zúñiga, S. Haro-Rodriguez, A. Santos-Beltrán, D. Ríos-Jara"Microstructure, transformation temperatures, hardness and magnetic properties of Co36.4+xNi33.3-xGa30.3 ferromagnetic SMA". *J. Alloys. Compd.*; vol. 499, no. 2, pp. 183-186, 2010.

[17] Elizabeth Jartych, J. K. Żurawicz, D. Oleszak, M. Pękaİa, "Hyperfine interactions, structure and magnetic properties of nanocrystalline Co-Fe-Ni alloys prepared by mechanical alloying", *Hyperfine Interactions*, vol. 168, no. 1, pp. 989-994, 2007.

[18] T.Nishizawa, K. Ishida, "The Co-Ni (Cobalt-Nickel) system" *Bull. Alloy. Phase. Diagr.*, vol. 4, no. 4, pp. 390–395, 1983.

[19] P. Taylor, R. Bauer, E. A. Jägle, W. Baumann, and E. Jan, "Kinetics of the allotropic hcp– fcc phase transformation in cobalt" *Philos. Mag.*, vol. 91, no. 3, pp. 437–457, 2011.

[20] F. Cardellini and G. Mazzone, "Thermal and structural study of the h.c.p.-to-f.c.c. transformation in cobalt" *Philos. Mag. A Phys. Condens. Matter, Struct. Defects Mech. Prop.*, vol. 67, no. 6, pp. 1289–1300, 1993.

[21] J. Sort, A. Zhilyaev, M. Zielinska, J. Nogues, S. Surinach, J. Thibault and M.D. Baro, "Microstructural effects and large microhardness in cobalt processed by high pressure torsion consolidation of ball milled powders" *Acta. Mater.*, vol. 51, no. 20, pp. 6385–6393, 2003.

[22] A. Mukhtar, T. Mehmood, and K. M. Wu, "Investigation of phase transformation of CoNi alloy nanowires at high potential Investigation of phase transformation of CoNi alloy nanowires at high potential" *Mater. Sci. Eng.*, vol. 239, pp. 12–17, 2017.

[23] Y.W. Cui, M. Jiang, I. Ohnuma, K. Oikawa, R. Kainuma, K. Ishida, “Computational study of atomic mobility for fcc phase of Co-Fe and Co-Ni binaries” *J. Phase. Equilibria. Diffus.*, vol. 29, no. 1, pp. 2–10, 2008.

[24] B. Neelima, N. V Rama Rao, V. Rangadhara Chary, and S. Pandian, “Influence of mechanical milling on structure , particle size , morphology and magnetic properties of rare earth free permanent magnetic Zr_2Co_{11} alloy” *J. Alloys. Compd.*, vol. 661, pp. 72–76, 2016.

[25] E. Fenineche, R. Hamzaoui, and O. El Kedim, “Structure and magnetic properties of nanocrystalline Co-Ni and Co-Fe mechanically alloyed” *Mater. Lett.*, vol. 57, no. 26–27, pp. 4165–4169, 2003.

[26] H. Shokrollahi, “The magnetic and structural properties of the most important alloys of iron produced by mechanical alloying” *Mater. Des.*, vol. 30, no. 9, pp. 3374–3387, 2009.

[27] C. Suryanarayana, *Mechanical Alloying and Milling,Materials Engineering, Marcel Dekker, NY*.2004.

[28] M. H. Enayati, G. R. Aryanpour, and A. Ebnonnasir, “Production of nanostructured WC-Co powder by ball milling” *Int. J. Refract. Met. Hard. Mater.*, vol. 27, no. 1, pp. 159–163, 2009.

[29] A. W. Weeber and H. Bakker, “Amorphization by ball milling. A review” *Phys. B Phys. Condens. Matter*, vol. 153, no. 1–3, pp. 93–135, 1988.

[30] A. Bahrami, H. R. M. Hosseini, P. Abachi, and S. Miraghaei, “Structural and soft magnetic properties of nanocrystalline $Fe_{85}Si_{10}Ni_5$ powders prepared by mechanical alloying” *Mater. Lett.*, vol. 60, no. 8, pp. 1068–1070, 2006.

[31] E. O. Hall, “The deformation and ageing of mild steel: II Characteristics of the Lüders deformation” *Proc. Phys. Soc. Sect. B*, vol. 64, no. 9, pp. 742–747, 1951.

[32] N. J. Petch, “The Cleavage Strength of Polycrystals,” *J. Iron. Steel. Inst.*, vol. 174, no. 19, pp. 25–28, 1953.

[33] R. Elkalkouli, M. Grosbras, and J. F. Dinhut, “Mechanical and magnetic properties of nanocrystallineFeCo alloys produced by mechanical alloying” *Nanostructured. Mater.*, vol. 5, no. 6, pp. 733–743, 1995.

[34] P. Elumalai, H. N. Vasan, M. Verelst, P. Lecante, V. Carles, and P. Tailhades, “Synthesis and characterization of sub-micron size Co-Ni alloys using malonate as precursor” *Mater. Res. Bull.*, vol. 37, no. 2, pp. 353–363, 2002

[35] P. Toneguzzo, G. Viau, O. Acher, F. Guillet, E. Bruneton, F. Vincent, F. Fievet, "CoNi and FeCoNi fine particles prepared by the polyol process: Physico-chemical characterization and dynamic magnetic properties" *J. Mater. Sci.*, vol. 35, pp. 3767–3784, 2002.

[36] M. Mhadhbi, M. Khitouni, L. Escoda, J. J. Suñol, and M. Dammak, "Characterization of mechanically alloyed nanocrystalline Fe(Al): Crystallite size and dislocation density" *J. Nanomater.*, vol. 2010.

[37] M. Khajepour and S. Sharafi, "Characterization of nanostructured Fe-Co-Si powder alloy" *Powder. Technol.*, vol. 232, pp. 124–133, 2012.

[38] S. Bergheul, A. Haddad, H. Tafat, and M. Azzaz, "Magnetic, microwave and absorbing properties Fe-Co of alloy synthesized by mechanical alloying process" *Int. J. Microstruct. Mater. Prop.*, vol. 1, pp. 334–340, 2006.

[39] B. Avar, M. Gogebakan, S. Ozcan, and S. Kerli, "Structural, mechanical and magnetic properties of Fe — 40-at.% Al powders during mechanical alloying" *J. Korean. Phys. Soc.*, vol. 65, no. 5, pp. 664–670, 2014.

[40] S. Olvera, J. Sánchez-marcos, F. J. Palomares, E. Salas, E. M. Arce, and P. Herrasti, "Characterization and corrosion behavior of CoNi alloys obtained by mechanical alloying" *Mater. Charact.*, vol. 93, pp. 79–86, 2014.

[41] M. E. McHenry and D. E. Laughlin, "Magnetic Properties of Metals and Alloys" in *Physical Metallurgy, fifth ed.*, vol. 1, Elsevier B.V., 2014, pp. 1881–2008.

[42] B.D. Cullity, C.D. Graham, *Introduction to Magnetic Materials, second ed.*, *IEEE Press, Wiley, Hoboken,* 2009.

[43] H. Shokrollahi, "The magnetic and structural properties of the most important alloys of iron produced by mechanical alloying" *Mater. Des.*, vol. 30, no. 9, pp. 3374–3387, 2009.

[44] B. Chitsazan, H. Shokrollahi, A. Behvandi, and M. Ghaffari, "Magnetic , structural and micro-structural properties of mechanically alloyed nano-structured $Fe_{48}Co_{48}V_4$ powder containing inter-metallic Co3V" *J. Magn. Magn. Mater.*, vol. 323, no. 9, pp. 1128–1133, 2011.

[45] R. Hamzaoui, O. Elkedim, E. Gaffet, and J. M. Greneche, "Structure, magnetic and Mössbauer studies of mechanically alloyed Fe-20 wt.% Ni powders" *J. Alloys. Compd.*, vol. 417, no. 1–2, pp. 32–38, 2006.

[46] C.W. Chen, *Magnetism and Metallurgy of Soft Magnetic Materials, North-Holland, Amsterdam,* 1977, pp. 132.

[47] Q. Zeng, I. Baker, V. McCreary, and Z. Yan, "Soft ferromagnetism in nanostructured mechanical alloying FeCo-based powders" *J. Magn. Magn. Mater.*, vol. 318, no. 1–2, pp. 28–38, 2007.

[48] R. Skomski, Simple Models of Magnetism, *Oxford University Press*, *NY*, Vol. 228, 2008, p. 3.

[49] H. Kronmüller and B. Gröger, "Domains , domain walls and the coercive field of amorphous ferromagnets" *J. Phys.*, vol. 42, no. 9, pp. 1285–1292, 1981.

[50] L. Dekhil, N. Zerniz, M. Bououdina, N. Haneche, E. B. Haneche, and J. M. Grenèche, "Characterization of bionanomaterial Ni_{60}-Cr_{40} alloy obtained by mechanical alloying" *J Mater. Environ.*, vol. 6, no. 7, pp. 1858–1864, 2015.

[51] B. Bhoi, V. Srinivas, and V. Singh, "Evolution of microstructure and magnetic properties of nanocrystalline $Fe_{70-x}Cu_xCo_{30}$ alloy prepared by mechanical alloying" *J. Alloys. Compd.*, vol. 496, no. 1–2, pp. 423–428, 2010.

[52] M. D. Chermahini, S. Sharafi, H. Shokrollahi, M. Zandrahimi, and A. Shafyei, "The evolution of heating rate on the microstructural and magnetic properties of milled nanostructured $Fe_{1-x}Co_x$ (x = 0.2 , 0.3 , 0.4 , 0.5 and 0 .7) powders" *J. Alloys. Compd.*, vol. 484, pp. 54–58, 2009.

[53] K. R. Pirota, M. Knobel, M. Hernandez-Velez, K. Nielsch, and M. Vazquez, "Magnetic Nanowires: Fabrication and Characterization" in *Oxford handbook of nanoscience and technology: materials: structures, properties and characterization techniques*, vol. 2, 2010, pp. 793.

[54] J. Sort, J. Nogués, S. Suriñach, J. S. Muñoz, and M. D. Baró, "Correlation between stacking fault formation, allotropic phase transformations and magnetic properties of ball-milled cobalt" *Mater. Sci. Eng.A*, vol. 377, pp. 869–873, 2004.

[55] A.Sato and M.Nagao, "Magnetic Properties of Dislocations" in *Encyclopedia of Materials: Science and Technology*, 2004, pp. 1–14.

[56] L. Piotrowski, M. Chmielewski, and Z. L. Kowalewski, "The Dominant Influence of Plastic Deformation Induced Residual Stress on the Barkhausen Effect Signal in Martensitic Steels" *J. Nondestruct. Eval.*, vol. 36, no. 1, pp. 1–8, 2017.

[57] J. S. Blazquez, V. Franco, C. F. Conde and A. Conde,, "Nanocrystalline Fe-Nb-(B,Ge) alloys from ball milling : Microstructure, thermal stability and magnetic properties" *Intermetallics*, vol. 15, pp. 1351–1360, 2007.

[58] I. Chicinas, "Soft magnetic nanocrystalline powders produced by mechanical alloying routes" *J. Optoelectron. Adv. Mater.*, vol. 8, no. 2, pp. 439–448, 2006.

[59] Y. Duan, Y. Zhang, T. Wang, S. Gu, L. Xin, and X. Lv, "Evolution study of microstructure and electromagnetic behaviors of Fe-Co-Ni alloy with mechanical alloying" *Mater. Sci. Eng. B Solid-State Mater. Adv. Technol.*, vol. 185, no. 1, pp. 86–93, 2014.

[60] Y. Jang Ik, J. Kim, and D. Shin Hyuk, "Microstructures and magnetic properties of amorphous Fe–Si–B–Ni alloy ribbons" *Mater. Sci. Eng. B*, vol. 78, pp. 113–118, 2000.

[61] R. Hamzaoui, O. Elkedim, N. Fenineche, and E. Gaffet, "Structure and magnetic properties of nanocrystalline mechanically alloyed Fe Á 10 % Ni and Fe Á 20 % Ni" *Mater. Sci. Eng. A*, vol. 360, pp. 299–305, 2003.

[62] M. DelshadChermahini, S. Sharafi, H. Shokrollahi, and M. Zandrahimi, "Microstructural and magnetic properties of nanostructured Fe and $Fe_{50}Co_{50}$ powders prepared by mechanical alloying" *J. Alloys. Compd.*, vol. 474, pp. 18–22, 2009.

[63] M. DelshadChermahini and H. Shokrollahi, "Milling and subsequent thermal annealing effects on the microstructural and magnetic properties of nanostructured $Fe_{90}Co_{10}$ and $Fe_{65}Co_{35}$ powders" *J. Alloys. Compd.*, vol. 480, pp. 161–166, 2009.

[64] A. Behvandi, H. Shokrollahi, B. Chitsazan, and M. Ghaffari, "Magnetic and structural studies of mechanically alloyed nanostructured $Fe_{49}Co_{49}V_2$ powders" *J. Magn. Magn. Mater.*, vol. 322, no. 24, pp. 3932–3937, 2010.

602

603

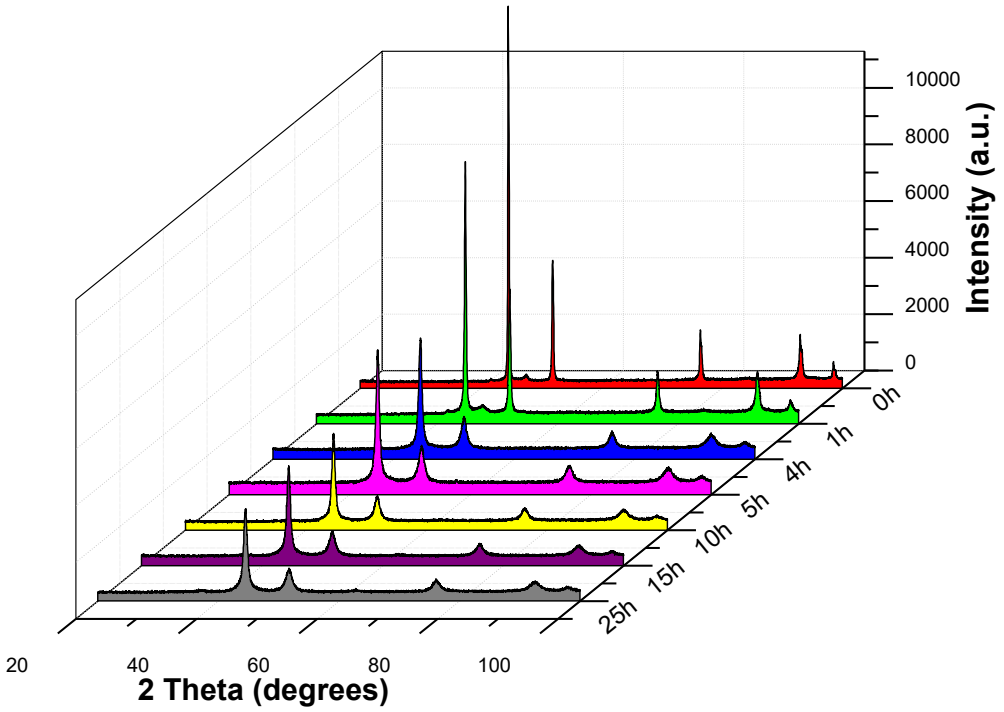

604

605

606

607

608 ***Figure 1.*** *Evolution of XRD patterns of MA* $Ni_{70}Co_{30}$ *powdersas function of milling time.*

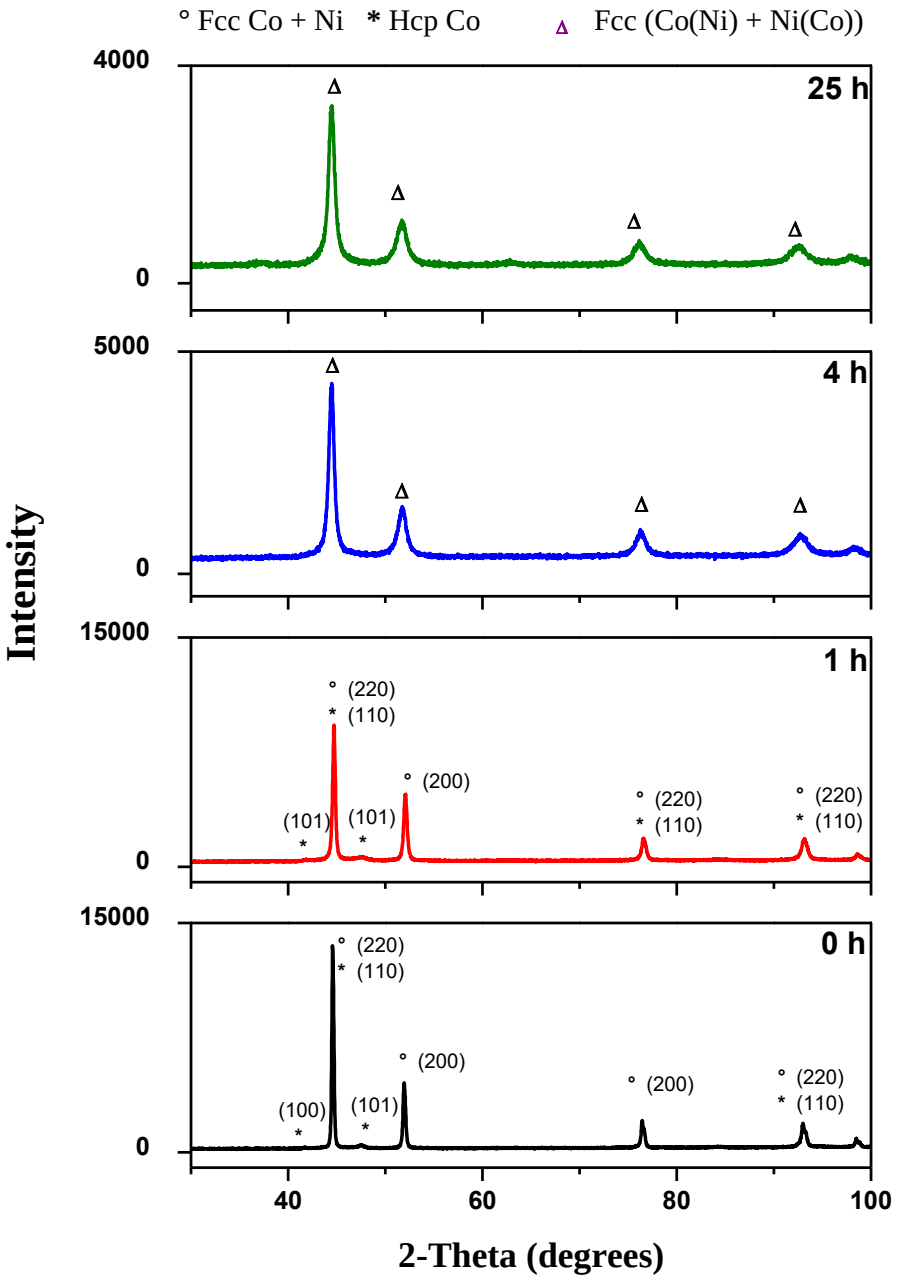

609

610 ***Figure 2.*** *XRD patterns of $Ni_{70}Co_{30}$ powders for different milling time (0 h, 1 h, 4 h and 25 h).*

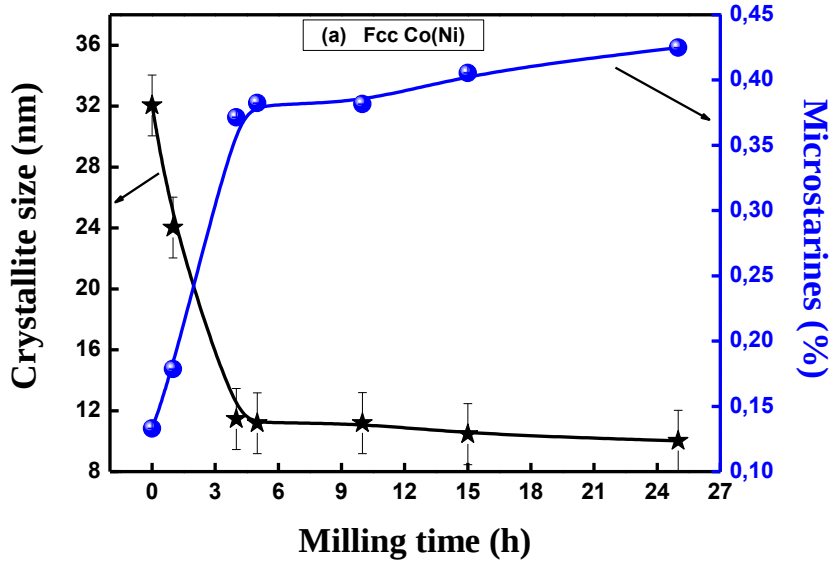

611

612

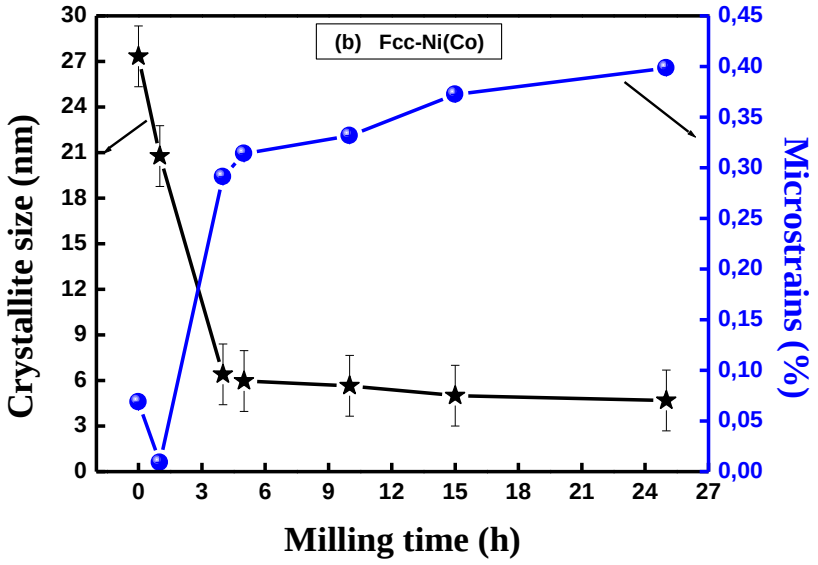

613

614

615

616 ***Figure 3.*** *Variation of crystallite size and microstrain with milling time: (a) fcc-Co(Ni) phase;(b)*
617 *fcc-Ni(Co) phase.*

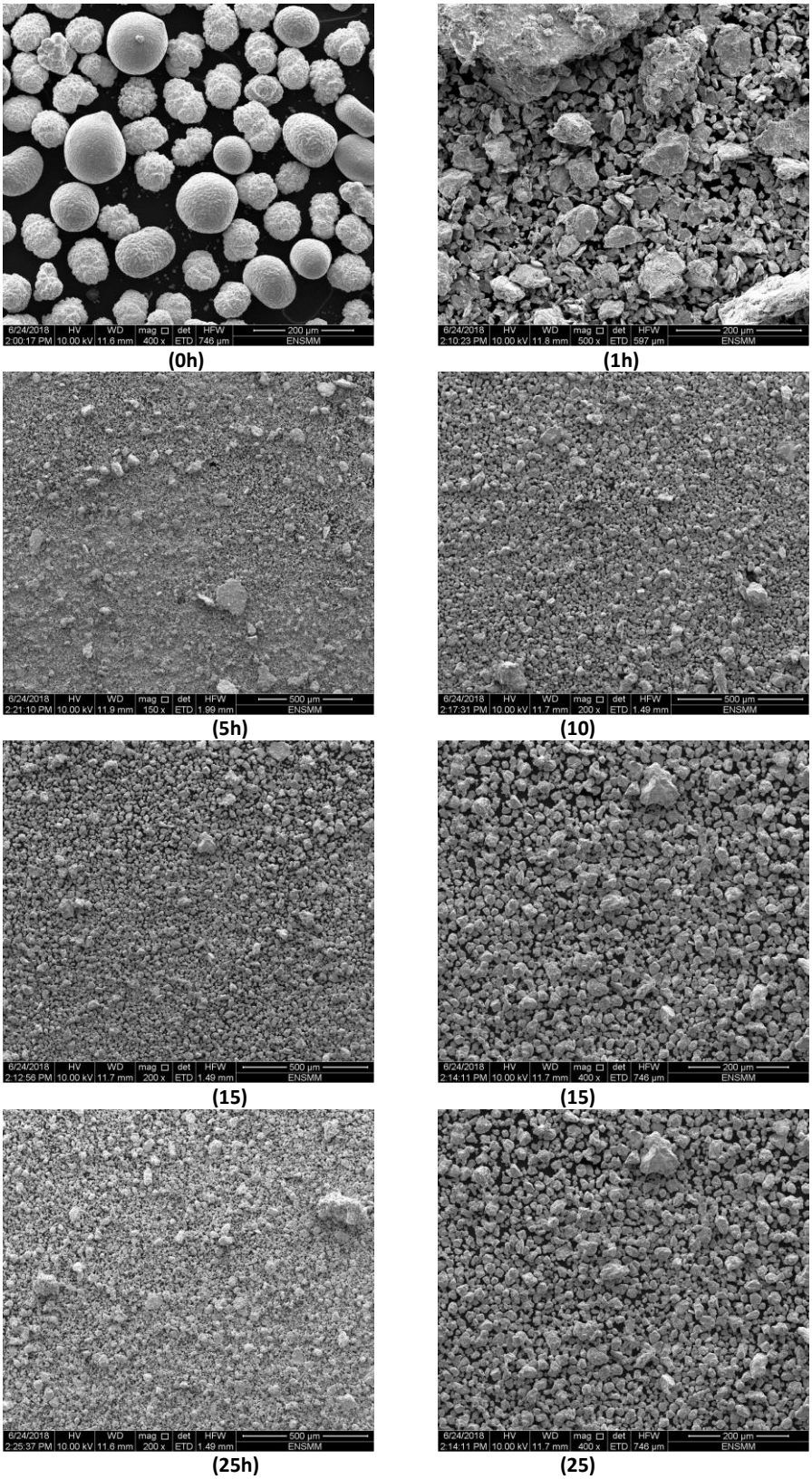

Figure 4. *SEM micrographs of MA $Ni_{70}Co_{30}$ powders.*

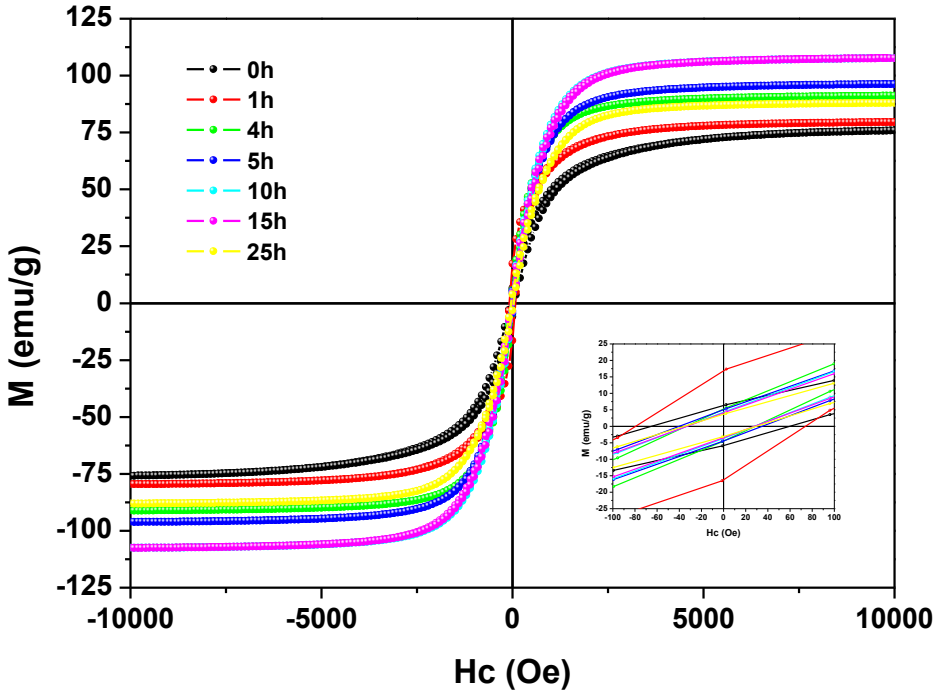

Figure 5. *Hysteresis loops recorded at T=300 K of MA $Ni_{70}Co_{30}$ powdersas a function of milling time.*

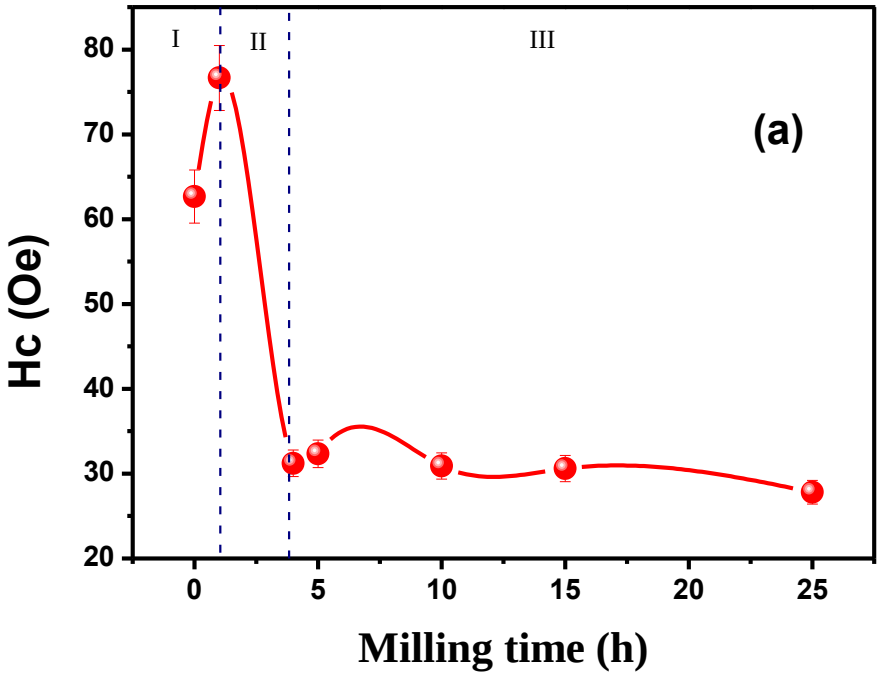

653

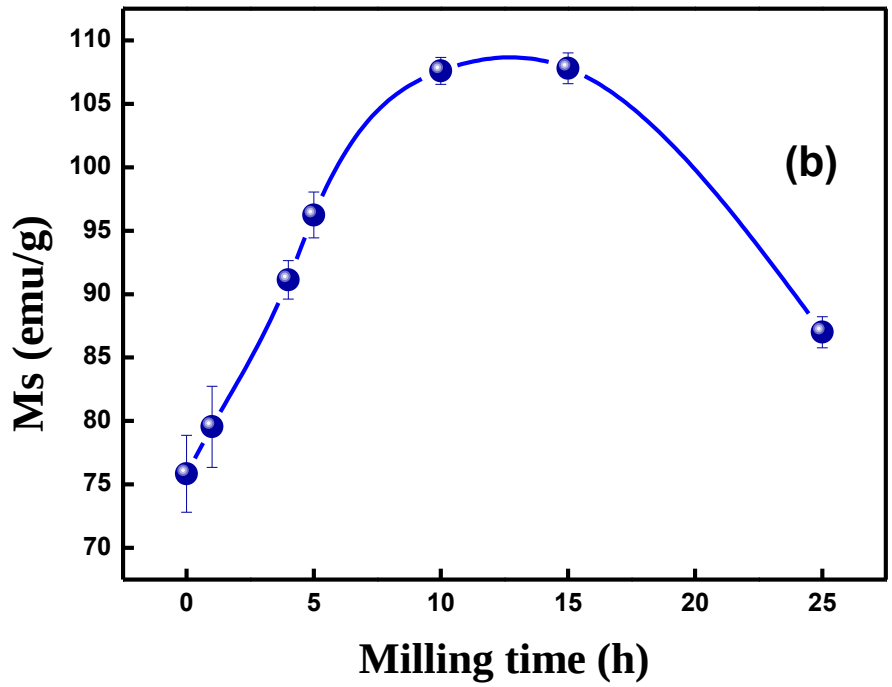

654

655 ***Figure 6.*** *Variation of (a) coercivity $H_{c,}$ and (b) saturation magnetization of MA $Ni_{70}Co_{30}$*
656 *powders as a function of milling time.*